Nano World Journal

http://dx.doi.org/10.17756/nwj.2015-006

Research Article

Open Access

Protein Crystallization by Anodic Porous Alumina (APA) Template: The Example of Hen Egg White Lysozyme (HEWL)

Eugenia Pechkova[1,2*], Nicola Luigi Bragazzi[1,2] and Claudio Nicolini[1,2,3]

[1]Biophysics and Nanobiotechnology Laboratories (BNL), Department of Experimental Medicine (DIMES), University of Genoa, Via Antonio Pastore 3, Genoa 16132, Italy
[2]Nanoworld Institute Fondazione EL.B.A Nicolini (FEN), Pradalunga, Largo Redaelli 7, Bergamo 24100, Italy
[3]European Synchrotron Radiation Facility (ESRF), Grenoble, 6 Rue Jules Horowitz 38000, France

[*]Correspondence to:
Professor Eugenia Pechkova
Laboratory Biophysics and Nanobiotechnology
Via Antonio Pastore 3
Genova, Italy
Tel: +3901035338217
E-mail: evgeniya.Pechkova@unige.it

Received: April 21, 2015
Accepted: May 19, 2015
Published: May 22, 2015

Citation: Pechkova E, Bragazzi NL, Nicolini C. 2015. Protein Crystallization by Anodic Porous Alumina (APA) Template: The Example of Hen Egg White Lysozyme (HEWL). *NanoWorld J* 1(2): 46-55.

Published by United Scientific Group

Abstract

In this communication, we report anodic porous alumina (APA) template induced crystallization. The APA nanotemplate was prepared on the glass substrate for the hen egg white lysozyme (HEWL) crystal growth. The changes in the lysozyme crystals morphology, namely in the a/c axis ratio, were observed in the crystal grown by APA nanotemplate, but not in the crystal obtained with classical hanging drop vapor diffusion method, under the same experimental conditions. The comparison of the diffraction data of the two crystals as well as bioinformatics and data mining approaches and molecular dynamics simulations suggest a possible explanation of the nanotemplate crystallization phenomenon and shed light on the APA-induced nanocrystallography.

Keywords

Anodic porous alumina (APA), Bioinformatics, Clustering, Data mining approach, Hen egg white lysozyme (HEWL), Heterogeneous crystallization, Molecular Dynamics (MD) simulation, Ordered template, Protein crystallization techniques

Introduction

Hen egg white lysozyme (HEWL) is a well-studied and easy to crystallize protein, which is widely used by researchers as a model protein both for testing novel crystallization methods and for improving existing crystal growth approaches, as well as for analytical and theoretical studies on the fundamental principles of crystallization and protein crystals properties. HEWL, besides enabling investigations on the relationship between structure and function, also represents an important model for clinical studies, especially in the field of amyloid research [1]. The most usually encountered crystallographic form of HEWL is the tetragonal space-group $P4_32_12$. The crystals grown by batch or classical vapor diffusion methods with NaCl solution as precipitate have this commonly known form [2]. Interestingly, it is well-known that the size and morphology of crystals can depend on various factors. Different researches have contributed to shed light on the critical parameters, such as precipitant concentration, buffer composition, pH, supersaturation and temperature [3, 4], high or low supersaturation condition [5] or contaminant concentration [6]. Moreover, some scholars have successfully managed to crystallize lysozyme using solid flat surfaces or templates, observing that the nature of each template has a peculiar influence on lysozyme crystal nucleation and growth [5]. For example, McPherson and collaborators (1988), pioneering heterogeneous crystallization, reported that protein crystals grew epitaxially on the surfaces of minerals [7]. In particular, McPherson and Shlichta

(1988) showed that at least 50 types of minerals can drive protein crystallization.

In order to control heterogeneous nucleation of lysozyme crystals, hair cuticles [8] or *ad hoc* engineered structured surfaces such as Poly-L-Lysine modified glass substrate [9], chemically modified mica surfaces [10] or other chemically modified patterns [11], xanthenes dyes [12], polystyrene nanospheres [13], porous glass [14], porous silicon [15] and fluorinated layered silicate (which is a phyllosilicate with a parallel two-dimensional lamellar structure; Ino et al., 2011) [16] can be exploited. In the last work, the fluorine atoms were considered responsible for driving the nucleation process. In the work by Chayen and collaborators [15], the authors found that a porous template with a porosity distribution in the range of 5-10 nm could properly act as a nucleating agent, in that, being the pores of a similar size to the proteins, they would entrap protein molecules, facilitating the formation and aggregation of ordered, crystalline structures [17]. Recently, the porosity distribution and pore size were proven as crucial parameters in induced heterogeneous nucleation of protein crystals in a porous medium by theoretical work using sophisticated mathematical models [18, 19] and advanced computational approaches, such as the Metropolis Monte Carlo algorithm [20].

Heterogeneous crystallization can help at least in the initial phases to find the optimal crystallization conditions and has proven to be an important advancement in macromolecular crystallography [17].

In our hands, nanobiothechnology-based templates were successful for inducing proper protein nucleation and crystallization [21]. In particular, nanobiotemplates consisting in Langmuir-Blodgett (LB) thin films of the protein chosen for the crystallization experiment cause acceleration and enhancement in the crystal growth, with a significantly increased crystal dimension [22], a greater resistance to radiation damage [23] and only minor, slight crystal structure changes [24, 25]. Moreover, LB-based crystallography can trigger the nucleation and crystallization of proteins never or rarely crystallized before, such as bovine cytochrome P450scc and human protein kinase CKII alpha subunit [26].

In this report, we present lysozyme crystallization obtained with anodic porous alumina (APA) nanotemplate, prepared by photolithographic microstructuring technique and two-step anodization process [27]. Due to its specific properties, the APA material could offer several advantages in biophysical and biochemical applications: high surface area enlargement, improved microfluidic properties, easy and cheap manufacturability, flexibility in porous dimension and mechanical straight enhancement [28]. It can be successfully used for immobilization of both oligonucleotides and DNA for design of gene micro-arrays and for immobilization of proteins, like cytochrome P450scc [28], for implementation of biosensors.

The new application of APA proposed in this article as a template material for enabling protein crystallization could give prominent results in control of crystal nucleation and growth as well as could improve crystal quality with the aim of determining and solving new macromolecular structures. The differences in HEWL crystal growth and crystal structure were studied comparing the crystal obtained with APA template with crystal obtained with classical hanging drop vapor diffusion method. Bioinformatics and molecular dynamics (MD) simulations were carried out in order to gain further insight on the influence of APA template on lysozyme crystal.

Experimental Section

Materials

APA template

Hexagonally ordered nanopore arrays with high aspect ratios based on a self-organization process in anodic alumina was fabricated. A two-step anodization technique [29] was used in order to oxidize aluminum in phosphoric acid solution. The task of evaporating alumina over glass has been accomplished by avoiding its detachment during the anodization process, a typical problem due to the incompatibility of cold borosilicate glass to the vapors of alumina. This phenomenon can be easily contrasted by means of a thin layer of chromium (deposited by sputtering) as medium element between glass and alumina. The ordered pore arrays are straight and parallel and with polycrystalline structure and a highly regular honeycomb distribution. The pore distance, pore density, pore depth, and wall thickness of APA template can be easily tuned and controlled by changing the anodic electrolyte and the applied voltage. The dielectric properties of Al_2O_3 make indeed this structure optimal for the realization of an electrically anisotropic system.

Two different lithographic micro-structuring techniques for the ordered nanopore arrays were reported in Grasso et al., 2005, using a positive resist and a negative resist leaving surface hydrophobic. The whole micro-structuring process is highly anisotropic and leads to a sharp edge (Figure 1a). The side walls of the structures are very steep, and their roughness is determined by the quality of the mask and the aluminum transfer layer. The whole process of APA template preparation is described in Stura et al., 2007 and Grasso et al., 2005. Briefly, alumina sheets were treated with a 1:4 (v:v) mixture of ethanol and perchloric acid for 3 minutes to clean the surface

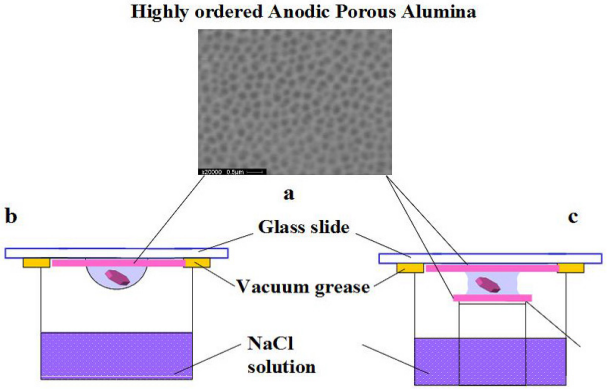

Figure 1: The APA template crystallization by hanging drop (b) and sandwich drop (c) modified techniques. Scanning electronic microscopy (SEM) picture (top view) showing highly ordered anodic porous alumina on the surface of the template, resulting at the end of photolithographic microstructuring technique and two- step anodization process (a), as described in the main text.

from impurities. Then, a first anodization process was carried out, in the cooling system and applying a current of 20 V using 1M oxalic acid as an electrolytic solution. Alumina sheets were connected as negative electrode and platinum sheets as positive electrode. The reaction was continued for 2 hours with vigorous stirring. Then the sample was rinsed with distilled water and treated with a mixture of phosphoric acid and chromium trioxide (1:4 v:v) to remove the first aluminum oxide layer. After this, a second electrolysis process was run for 30 minutes. Morphological parameters of anodic porous alumina, like mean pore diameter, pore density were determined by the image analysis of the atomic force microscopy (AFM) scanning. The porosity was obtained from the ratio: Porosity % = (S_{pore}/S_{wall}) X 100 where S_{pore} is the surface area of pores and S_{wall} is the oxide geometric surface.

Our APA template consisted of spot 120–500 μm wide, and 20–100 μm high.

APA template crystallization method

HEWL was purchased by Sigma.

Similarly to LB-based nanotemplate crystallization method, the APA template, prepared on the glass cover slide, was used in the protein hanging drop crystallization well in such a way to put the droplet of protein solution in contact with the nanotemplate (Figure 1b). For the sandwich drop experiment, the wells were prepared with two APA nanotemplates (Figure 1c). A 4 ml drop containing 40 mg/ml of HEWL solution in 50 mM sodium acetate buffer pH 4.5 was mixed with 2 ml of 0.9M NaCl solution and equilibrated on the reservoir, containing the salt solution. The classical hanging and sandwich drop experiments were carried out in parallel, using the same experimental crystallization condition. We used the Olympus light microscope with 100 times magnification for the crystal measurement.

Data collection and processing

Diffraction data were collected at a temperature of 100° K at the European Synchrotron Radiation Facility (ESRF) at the microfocus beamline ID13 (beam 20 X 20 μm). Crystals were fished out from the mother liquor and frozen in a nitrogen stream using Paraton-N (Hampton Research) as cryoprotectant. The wavelength used was 0.9755 Å and the crystal to MAR CCD detector distance was 100 mm. Crystals diffracted to a maximum resolution of 1.6-1.7 Å.

Standard procedures of data reduction were followed using programs from the CCP4 suite, MOSFLM and SCALA. The phase problem was solved using the molecular replacement method, using the software package CNS and the three-dimensional structures were determined from the electron-density map, using the software packages QUANTA (via map skeletonization and secondary-structure determination) and the package XtalView (via direct fitting of C^{α} atoms). Refinement was performed manually using both packages, followed by automatic restrained refinement with isotropic B factors, using the CCP4 suite program REFMAC5.

APA-based HEWL crystal has been deposited in Protein Data Bank (PDB) as 3IJU, while the classical lysozyme as 3IJV.

Modeling

Bioinformatics and data-mining

In order to compare our APA-obtained crystal (PDB code *3IJU*) with other crystals from the PDB repository [30], we extensively exploited bioinformatics and data-mining approaches. This method was already successfully used to study LB- and space-grown crystals [31]. 53 structures deposited in PDB obtained in the same range of experimental conditions (pH, temperature, pressure) but with different techniques of crystallization have been structurally aligned using ProCKSI server [32]. The most accurate method of 3D protein structure alignment TMalign [33] was used, and root mean square deviations for C-alpha atoms were used as the similarity measure for all structures.

Protein domains alignment was done using STRAP software (Table 2).

Molecular dynamics simulation

MD simulation was performed using the CABS-flex server [34]. Movies of the proteins MD simulations can be found as supplementary material (in MP4 format).

Results and Discussion

The typical APA sample obtained by using the APA microstructuring process is shown in (Figure 1c). Hexagonally ordered pore domains were prepared by a self-organization process under specific anodization conditions. This micropatterning technique leads to a sharp edge. The anisotropy of the process can be seen with the focused ion beam (FIB) set-up (Figure 2a). The sidewalls of the structures are very steep, and their roughness is determined by the quality of the mask. This second resist having hydrophobic properties increases specificity to biological sample linking.

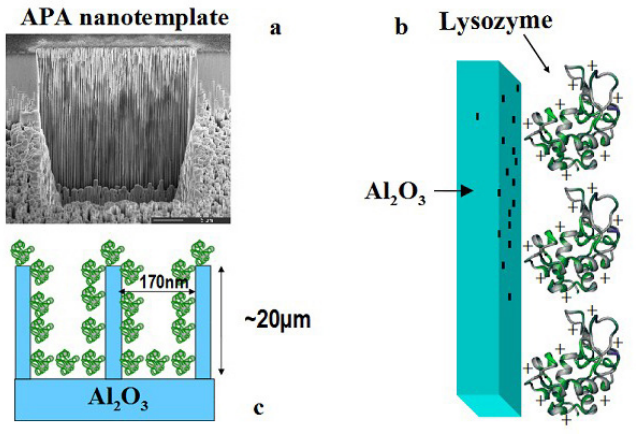

Figure 2: : The schematic picture of the anodic porous alumina (APA) template: the lysozyme molecules on the aluminum oxide surface (b); FIB system images of cross-sectional morphologies of the microarray spot, resulting at the end of photolithographic microstructuring technique and two-step anodization process (focused ion beam set-up or FIB system allows to see the anisotropy of the process) (a) and schematic sketch of the APA template in the contact with protein solution (c).

We analyzed the morphology of a large number of crystals, performing more than two hundred trials. The APA-grown crystal (PDB code 3IJU) demonstrates a different form in

comparison with the crystal obtained with the classical method (PDB code 3IJV), in particular in the crystal elongation. This effect was already observed by Durbin and Feher (1986) [35], who reported that the growth rates of the {110} and {101} faces have a different concentration dependence, resulting in an elongation of the crystal at lower lysozyme concentrations. Later, it was found that this could depend on various parameter, including pH, temperature, supersaturation, but the most consistent trend was associated with the pH variation. Other scholars found that a contaminant effect could lead to a shortening along the c axis of the crystal, depending on the contaminant concentration [6] In our case, morphology measurements indicate a putative APA template effect leading to an elongation along the c axis (the distance between the apexes of the {101} faces) and shortening along the a axis (the distance between parallel {110} faces) of the crystal.

A sketch of the general shape of the crystal morphology is shown on the (Figure 3). The measurement of interest is the ratio of the length of the horizontal axis/dotted line (defined as '*c*') to the length of the vertical axis/dotted line (defined as '*a*'). The change in this axial ratio was observed for the crystals obtained by the APA template in comparison with the crystals grown by classical hanging drop vapor diffusion method. In case of classical crystals this ratio is 1.58, while in case of the crystals grown by APA nanotemplate, is 5.84. The same phenomenon was observed in the case of the sandwich drop method, where the crystal were grown in between of two APA templates (see Figure 1c): considering all the crystallization trials we performed, the axial ratio shows a definite increasing trend in the presence of APA nanotemplate, while the number of crystals in the drops was decreased (Figure 4).

This result appears to be interesting, since all other

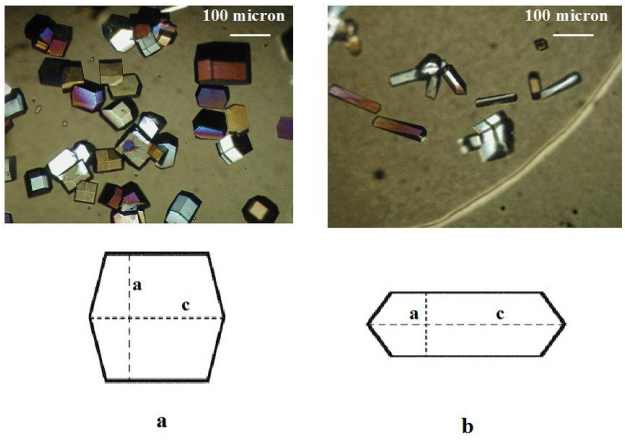

Figure 3: Lysozyme crystals produced classical hanging drop method (a) and by APA template described in Figure 1a (b) with their respective schematic pictures.

parameters (pH, temperature, supersaturation) were the same for both classical and APA template-based crystallization process. Moreover, the crystal size (defined as the distance between parallel {110} faces) remains the same for both classical and APA template-grown crystals. Thereby, the APA template reproducibly influences the HEWL crystal morphology, causing decreasing of *a*/*c* ratio, which was confirmed by performing over 100 crystals optical measurements.

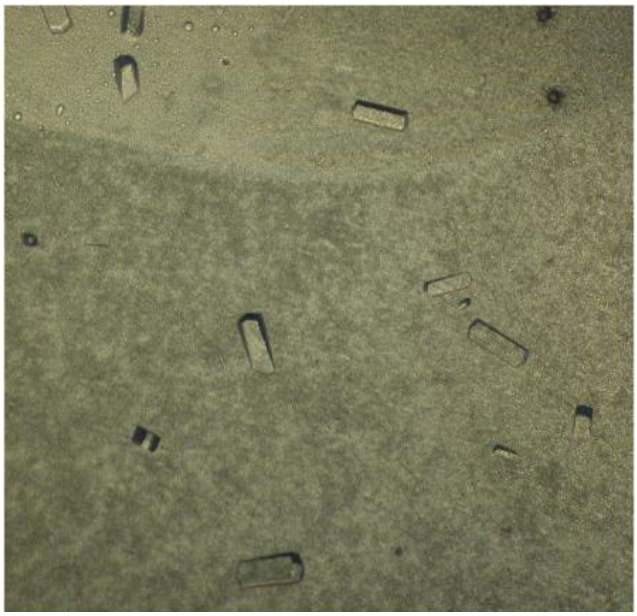

Figure 4: Lysozyme crystals produced by APA template sandwich drop method described in Figure 1c.

It is well known that the foreign surfaces can enhance the formation of nuclei, e.g. in the same supersaturation conditions the nucleation occur preferably on the solid surface rather than in the homogeneous phase. This phenomena has the thermodynamic nature and related with adhesion. In general, the immersed solid material surface decreases the activation energy for nucleation through the reduced interfacial free energy between the nucleus and the wet solid surface. Thus, it should be possible to influence the nucleation by selectively varying the nature of the liquid-solid interface. In this case, APA surface appear to influence the protein nucleation and growth as it is clear from crystal morphology. Since that APA surface is negatively charged, it could attract the lysozyme molecules, which have the mostly positive charges on its surface (Figure 2b). Generally, adsorption of charged proteins onto an oppositely charged surface, in particular lysozyme on mica is well known and studied [36, 37]. Thus, highly ordered pattern of APA can produce the same highly ordered lysozyme pattern which can favor the nucleation and crystallization in the specific way (Figure 2c). Next, being porous material, APA can trig the nucleation inside the pores. In this case, the space restriction factor cam take place, causing the elongation of the c-axis of the crystal.

From the diffraction data analysis, the structure of the crystal grown with APA template seems to be similar to classical lysozyme structure, and have the same space-group symmetry. Some slight differences, however, can be observed. For example, from a structural point of view, if studying the secondary structure, we can notice some differences in terms of helix content, which appears to be increased in the case of APA crystals (Figure 5). However, this reflects the range of variability of the studied structures included in our bioinformatics study (Table 2) and confirms our previous articles and the hypothesis that nanobiotechnology-based protein crystals have only minor or not significant structural changes in comparison with the classical crystals [24, 25].

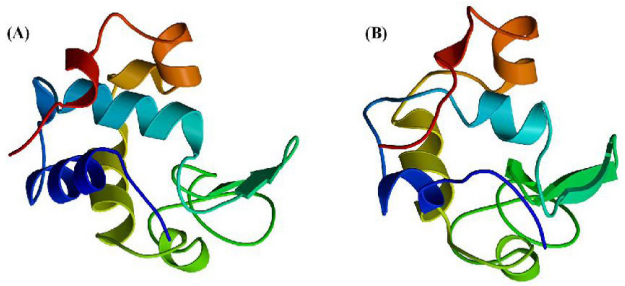

Figure 5: Comparison of lysozyme crystal structure obtained by anodic porous alumina (APA) template (a) and classical hanging drop (b). all the helices appear constantly more pronounced in the case of APA induced lysozyme crystal.

The unit cell parameters are also slightly changed in the case of APA in comparison to the classical crystal, namely the cell volume is slightly increased (Table 1).

Moreover, the quality of crystals appears to be higher in the case of APA, than those grown by classical hanging drop.

Table 1: The data collection statistics and analysis of APA-grown vs classical hanging drop crystal structure.

Crystallographical parameters	**APA-grown crystal (*3IJU*)**	**Classical crystal (*3IJV*)**
Resolution range (Å)	1.60-21.57	1.70-26.26
Unit cell parameters a,c (where a=b) (Å) α=β=γ (°) Group symmetry	 79.06, 37.54 90.00 P 4_3 2_1 2	 76.47, 36.12 90.00 P 4_3 2_1 2
Completeness (%)	97.8	88.5
R-factor	0.226	0.226
R_{free}	0.237	0.264
Mean isotropic B-factor	18.645	13.076
Ramachandran outliers (%)	0.0	0.0
I/Sigma	1.5	6.5
Number of water molecules	215	227
Number of unique reflections	16,005	11,287
Cell Volume (Å^3)	234,643.154	211,217.512
Structural parameters	**APA-grown crystal (*3IJU*)**	**Classical crystal (*3IJV*)**
RMS bonds (Å)	0.011	0.012
Helix content (%)	59	55
Coil content (%)	14	13
Strands content (%)	8	8
Turns content (%)	44	49

Indeed, the crystal grown in the presence of APA surface has the higher diffraction quality (see Table 1) and diffracts to the maximum resolution of 1.6 Å while classical crystal diffracts to 1.7 Å, with the intensity of diffraction of the APA-based crystal being higher in comparison with the classical one, even though the mean isotropic B-factor of *3IJU* is higher than the value of *3IJV* (see Table 1). The other crystallographical parameters are comparable (see Table 1). However, this is in accord with the previous research on LB nanotemplate crystallization method, which seems to produce higher quality, radiation stable lysozyme crystals [38].

Using insights from bioinformatics and data-mining, it is noteworthy to see that our APA-grown crystal does not cluster together with the classical one of comparison (Figure 6) and, intriguingly, that our APA lysozyme is more similar to those structures obtained via nanobiotechnologies (namely gold nanoparticles assisted *in situ* growth), suggesting a common physical mechanism (Figure 7). The classical crystal indeed differs the most from our APA-crystal (Table 3, Figure 8).

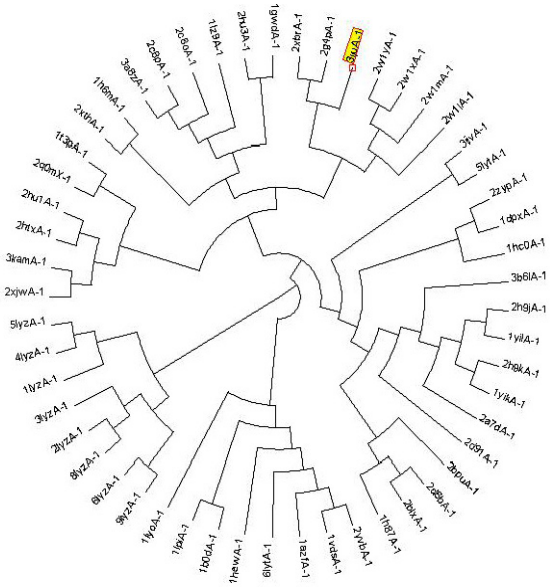

Figure 6: Clustering radial tree of the PDB compared structures, performed with PROCKSI server, as described in the main text.

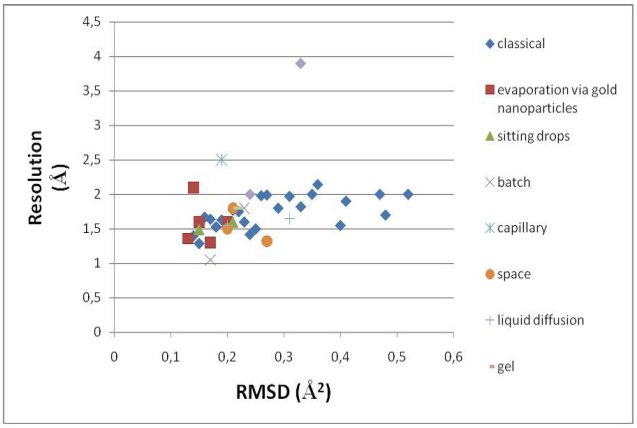

Figure 7: All the included lysozyme structures deposited in the Protein Data Bank (PDB) are plotted according to their resolution and their RMSD values. The nanobiotechnologies-based crystals are the most similar in the structural alignment and resolution (namely, APA-obtained and gold nanoparticles ones). Abbreviations: Classical: hanging drop vapor diffusion method; evaporation via gold nanoparticles: gold nanoparticles assisted *in situ* growth; sitting drops: modified hanging drop vapor diffusion sitting drop variant; batch: batch and micro-batch protein crystallization; capillary: capillary protein crystallization; space: protein crystallization under microgravity condition; liquid diffusion: gel: gel protein crystallization.

Table 2: 53 lysozymes from PDB as explained in the text have been structurally compared using STRAP software for investigating their secondary structure. Helices and beta sheets have respectively a red and yellow background.

pdb6lyz KVFGRCELAAAMKRHGLDNYRGYSLGNWVCAAKFESNFNTQATNRNTDGSTDYGILQINSRWWCND-
GRTPGSRNLCNIPCSALLSSDITASVNCAKKIVSDGNGMNAWVAWRNRCKGTDVQAWIRGCRL

pdb5lyz KVFGRCELAAAMKRHGLDNYRGYSLGNWVCAAKFESNFNTQATNRNTDGSTDYGILQINSRWWCND-
GRTPGSRNLCNIPCSALLSSDITASVNCAKKIVSDGNGMNAWVAWRNRCKGTDVQAWIRGCRL

pdb4lyz KVFGRCELAAAMKRHGLDNYRGYSLGNWVCAAKFESNFNTQATNRNTDGSTDYGILQINSRWWCND-
GRTPGSRNLCNIPCSALLSSDITASVNCAKKIVSDGNGMNAWVAWRNRCKGTDVQAWIRGCRL

pdb3lyz KVFGRCELAAAMKRHGLDNYRGYSLGNWVCAAKFESNFNTQATNRNTDGSTDYGILQINSRWWCND-
GRTPGSRNLCNIPCSALLSSDITASVNCAKKIVSDGNGMNAWVAWRNRCKGTDVQAWIRGCRL

pdb2lyz KVFGRCELAAAMKRHGLDNYRGYSLGNWVCAAKFESNFNTQATNRNTDGSTDYGILQINSRWWCND-
GRTPGSRNLCNIPCSALLSSDITASVNCAKKIVSDGNGMNAWVAWRNRCKGTDVQAWIRGCRL

pdb1lyz KVFGRCELAAAMKRHGLDNYRGYSLGNWVCAAKFESNFNTQATNRNTDGSTDYGILQINSRWWCND-
GRTPGSRNLCNIPCSALLSSDITASVNCAKKIVSDGNGMNAWVAWRNRCKGTDVQAWIRGCRL

pdb8lyz KVFGRCELAAAMKRHGLDNYRGYSLGNWVCAAKFESNFNTQATNRNTDGSTDYGILQINSRWWCND-
GRTPGSRNLCNIPCSALLSSDITASVNCAKKIVSDGNGMNAWVAWRNRCKGTDVQAWIRGCRL

pdb9lyz KVFGRCELAAAMKRHGLDNYRGYSLGNWVCAAKFESNFNTQATNRNTDGSTDYGILQINSRWWCND-
GRTPGSRNLCNIPCSALLSSDITASVNCAKKIVSDGNGMNAWVAWRNRCKGTDVQAWIRGCRL

pdb6lyt KVFGRCELAAAMKRHGLDNYRGYSLGNWVCAAKFESNFNTQATNRNTDGSTDYGILQINSRWWCND-
GRTPGSRNLCNIPCSALLSSDITASVNCAKKIVSDGNGMNAWVAWRNRCKGTDVQAWIRGCRL

pdb5lyt KVFGRCELAAAMKRHGLDNYRGYSLGNWVCAAKFESNFNTQATNRNTDGSTDYGILQINSRWWCND-
GRTPGSRNLCNIPCSALLSSDITASVNCAKKIVSDGNGMNAWVAWRNRCKGTDVQAWIRGCRL

pdb1hew KVFGRCELAAAMKRHGLDNYRGYSLGNWVCAAKFESNFNTQATNRNTDGSTDYGILQINSRWWCND-
GRTPGSRNLCNIPCSALLSSDITASVNCAKKIVSDGNGMNAWVAWRNRCKGTDVQAWIRGCRL

pdb1azf KVFGRCELAAAMKRHGLDNYRGYSLGNWVCAAKFESNFNTQATNRNTDGSTDYGILQINSRWWCND-
GRTPGSRNLCNIPCSALLSSDITASVNCAKKIVSDGNGMNAWVAWRNRCKGTDVQAWIRGCRL

pdb1lyo KVFGRCELAAAMKRHGLDNYRGYSLGNWVCAAKFESNFNTQATNRNTDGSTDYGILQINSRWWCND-
GRTPGSRNLCNIPCSALLSSDITASVNCAKKIVSDGNGMNAWVAWRNRCKGTDVQAWIRGCRL

pdb1lpi KVFGRCELAAAMKRHGLDNYRGYSLGNWVCAAKFESNFNTQATNRNTDGSTDYGILQINSRWWCND-
GRTPGSRNLCNIPCSALLSSDITASVNCAKKIVSDGNGMNAWVAWRNRCKGTDVQAWIRGCRL

pdb1b0d KVFGRCELAAAMKRHGLDNYRGYSLGNWVCAAKFESNFNTQATNRNTDGSTDYGILQINSRWWCND-
GRTPGSRNLCNIPCSALLSSDITASVNCAKKIVSDGNGMNAWVAWRNRCKGTDVQAWIRGCRL

pdb1lz9 KVFGRCELAAAMKRHGLDNYRGYSLGNWVCAAKFESNFNTQATNRNTDGSTDYGILQINSRWWCND-
GRTPGSRNLCNIPCSALLSSDITASVNCAKKIVSDGNGMNAWVAWRNRCKGTDVQAWIRGCRL

pdb1dpx KVFGRCELAAAMKRHGLDNYRGYSLGNWVCAAKFESNFNTQATNRNTDGSTDYGILQINSRWWCND-
GRTPGSRNLCNIPCSALLSSDITASVNCAKKIVSDGNGMNAWVAWRNRCKGTDVQAWIRGCRL

pdb1h6m KVFGRCELAAAMKRHGLDNYRGYSLGNWVCAAKFQSNFNTQATNRNTDGSTDYGILQINSRWWCND-
GRTPGSRNLCNIPCSALLSSDITASVNCAKKIVSDGNGMNAWVAWRNRCKGTDVQAWIRGCRL

pdb1h87 KVFGRCELAAAMKRHGLDNYRGYSLGNWVCAAKFESNFNTQATNRNTDGSTDYGILQINSRWWCND-
GRTPGSRNLCNIPCSALLSSDITASVNCAKKIVSDGNGMNAWVAWRNRCKGTDVQAWIRGCRL

pdb1gwd KVFGRCELAAAMKRHGLDNYRGYSLGNWVCAAKFESNFNTQATNRNTDGSTDYGILQINSRWWCND-
GRTPGSRNLCNIPCSALLSSDITASVNCAKKIVSDGNGMNAWVAWRNRCKGTDVQAWIRGCRL

pdb1vds KVFGRCELAAAMKRHGLDNYRGYSLGNWVCAAKFESNFNTQATNRNTDGSTDYGILQINSRWWCND-
GRTPGSRNLCNIPCSALLSSDITASVNCAKKIVSDGNGMNAWVAWRNRCKGTDVQAWIRGCRL

pdb1yil KVFGRCELAAAMKRHGLDNYRGYSLGNWVCAAKFESNFNTQATNRNTDGSTDYGILQINSRWWCND-
GRTPGSRNLCNIPCSALLSSDITASVNCAKKIVSDGNGMNAWVAWRNRCKGTDVQAWIRGCRL

pdb1yik KVFGRCELAAAMKRHGLDNYRGYSLGNWVCAAKFESNFNTQATNRNTDGSTDYGILQINSRWWCND-
GRTPGSRNLCNIPCSALLSSDITASVNCAKKIVSDGNGMNAWVAWRNRCKGTDVQAWIRGCRL

```
pdb2a7d      KVFGRCELAAAMKRHGLDNYRGYSLGNWVCAAKFESNFNTQATNRNTDGSTDYGILQINSRWWCND-
GRTPGSRNLCNIPCSALLSSDITASVNCAKKIVSDGNGMNAWVAWRNRCKGTDVQAWIRGCRL

pdb1t3p      KVFGRCELAAAMKRHGLDNYRGYSLGNWVCAAKFESNFNTQATNRNTDGSTDYGILQINSRWWCND-
GRTPGSRNLCNIPCSALLSSDITASVNCAKKIVSDGNGMNAWVAWRNRCKGTDVQAWIRGCRL

pdb2blx      KVFGRCELAAAMKRHGLDNYRGYSLGNWVCAAKFESNFNTQATNRNTDGSTDYGILQINSRWWCND-
GRTPGSRNLCNIPCSALLSSDITASVNCAKKIVSDGNGMNAWVAWRNRCKGTDVQAWIRGCRL

pdb1hc0      KVFGRCELAAAMKRHGLDNYRGYSLGNWVCAAKFESNFNTQATNRNTDGSTDYGILQINSRWWCND-
GRTPGSRNLCNIPCSALLSSDITASVNCAKKIVSDGNGMNAWVAWRNRCKGTDVQAWIRGCRL

pdb2d6b      KVFGRCELAAAMKRHGLDNYRGYSLGNWVCAAKFESNFNTQATNRNTDGSTDYGILQINSRWWCND-
GRTPGSRNLCNIPCSALLSSDITASVNCAKKIVSDGNGMNAWVAWRNRCKGTDVQAWIRGCRL

pdb2c8p      KVFGRCELAAAMKRHGLDNYRGYSLGNWVCAAKFESNFNTQATNRNTDGSTDYGILQINSRWWCND-
GRTPGSRNLCNIPCSALLSSDITASVNCAKKIVSDGNGMNAWVAWRNRCKGTDVQAWIRGCRL

pdb2c8o      KVFGRCELAAAMKRHGLDNYRGYSLGNWVCAAKFESNFNTQATNRNTDGSTDYGILQINSRWWCND-
GRTPGSRNLCNIPCSALLSSDITASVNCAKKIVSDGNGMNAWVAWRNRCKGTDVQAWIRGCRL

pdb2d91      KVFGRCELAAAMKRHGLDNYRGYSLGNWVCAAKFESNFNTQATNRNTDGSTDYGILQINSRWWCND-
GRTPGSRNLCNIPCSALLSSDITASVNCAKKIVSDGNGMNAWVAWRNRCKGTDVQAWIRGCRL

pdb2bpu      KVFGRCELAAAMKRHGLDNYRGYSLGNWVCAAKFESNFNTQATNRNTDGSTDYGILQINSRWWCND-
GRTPGSRNLCNIPCSALLSSDITASVNCAKKIVSDGNGMNAWVAWRNRCKGTDVQAWIRGCRL

pdb2g4p      KVFGRCELAAAMKRHGLDNYRGYSLGNWVCAAKFESNFNTQATNRNTDGSTDYGILQINSRWWCND-
GRTPGSRNLCNIPCSALLSSDITASVNCAKKIVSDGNGMNAWVAWRNRCKGTDVQAWIRGCRL

pdb2h9k      KVFGRCELAAAMKRHGLDNYRGYSLGNWVCAAKFESNFNTQATNRNTDGSTDYGILQINSRWWCND-
GRTPGSRNLCNIPCSALLSSDITASVNCAKKIVSDGNGMNAWVAWRNRCKGTDVQAWIRGCRL

pdb2h9j      KVFGRCELAAAMKRHGLDNYRGYSLGNWVCAAKFESNFNTQATNRNTDGSTDYGILQINSRWWCND-
GRTPGSRNLCNIPCSALLSSDITASVNCAKKIVSDGNGMNAWVAWRNRCKGTDVQAWIRGCRL

pdb2yvb      KVFGRCELAAAMKRHGLDNYRGYSLGNWVCAAKFESNFNTQATNRNTDGSTDYGILQINSRWWCND-
GRTPGSRNLCNIPCSALLSSDITASVNCAKKIVSDGNGMNAWVAWRNRCKGTDVQAWIRGCRL

pdb2hu1      KVFGRCELAAAMKRHGLDNYRGYSLGNWVCAAKFESNFNTQATNRNTDGSTDYGILQINSRWWCND-
GRTPGSRNLCNIPCSALLSSDITASVNCAKKIVSDGNGMNAWVAWRNRCKGTDVQAWIRGCRL

pdb2htx      KVFGRCELAAAMKRHGLDNYRGYSLGNWVCAAKFESNFNTQATNRNTDGSTDYGILQINSRWWCND-
GRTPGSRNLCNIPCSALLSSDITASVNCAKKIVSDGNGMNAWVAWRNRCKGTDVQAWIRGCRL

pdb2hu3      KVFGRCELAAAMKRHGLDNYRGYSLGNWVCAAKFESNFNTQATNRNTDGSTDYGILQINSRWWCND-
GRTPGSRNLCNIPCSALLSSDITASVNCAKKIVSDGNGMNAWVAWRNRCKGTDVQAWIRGCRL

pdb2q0m      KVFGRCELAAAMKRHGLDNYRGYSLGNWVCAAKFESNFNTQATNRNTDGSTDYGILQINSRWWCND-
GRTPGSRNLCNIPCSALLSSDITASVNCAKKIVSDGNGMNAWVAWRNRCKGTDVQAWIRGCRL

pdb3b6l     KVFGRCELAAAMKRHGLDNYRGYSLGNWVCAAKFESNFNTQATNRNTDGSTDYGILQINSRWWCND-
GRTPGSRNLCNIPCSALLSSDITASVNCAKKIVSDGNGMNAWVAWRNRCKGTDVQAWIRGCRL

pdb2w1l      KVFGRCELAAAMKRHGLDNYRGYSLGNWVCAAKFESNFNTQATNRNTDGSTDYGILQINSRWWCND-
GRTPGSRNLCNIPCSALLSSDITASVNCAKKIVSDGNGMNAWVAWRNRCKGTDVQAWIRGCRL

pdb2w1x      KVFGRCELAAAMKRHGLDNYRGYSLGNWVCAAKFESNFNTQATNRNTDGSTDYGILQINSRWWCND-
GRTPGSRNLCNIPCSALLSSDITASVNCAKKIVSDGNGMNAWVAWRNRCKGTDVQAWIRGCRL

pdb2w1m      KVFGRCELAAAMKRHGLDNYRGYSLGNWVCAAKFESNFNTQATNRNTDGSTDYGILQINSRWWCND-
GRTPGSRNLCNIPCSALLSSDITASVNCAKKIVSDGNGMNAWVAWRNRCKGTDVQAWIRGCRL

pdb2w1y      KVFGRCELAAAMKRHGLDNYRGYSLGNWVCAAKFESNFNTQATNRNTDGSTDYGILQINSRWWCND-
GRTPGSRNLCNIPCSALLSSDITASVNCAKKIVSDGNGMNAWVAWRNRCKGTDVQAWIRGCRL

pdb2zyp      KVFGRCELAAAMKRHGLDNYRGYSLGNWVCAAKFESNFNTQATNRNTDGSTDYGILQINSRWWCND-
GRTPGSRNLCNIPCSALLSSDITASVNCAKKIVSDGNGMNAWVAWRNRCKGTDVQAWIRGCRL

pdb3kam      KVFGRCELAAAMKRHGLDNYRGYSLGNWVCAAKFESNFNTQATNRNTDGSTDYGILQINSRWWCND-
GRTPGSRNLCNIPCSALLSSDITASVNCAKKIVSDGNGMNAWVAWRNRCKGTDVQAWIRGCRL
```

```
LCNIPCSALLSSDITASVNCAKKIVSDGNGMNAWVAWRNRCKGTDVQAWIRGCRL

pdb3ijv      KVFGRCELAAAMKRHGLDNYRGYSLGNWVCAAKFESNFNTQATNRNTDGSTDYGILQINSRWWCND-
GRTPGSRNLCNIPCSALLSSDITASVNCAKKIVSDGNGMNAWVAWRNRCKGTDVQAWIRGCRL

pdb3iju      KVFGRCELAAAMKRHGLDNYRGYSLGNWVCAAKFESNFNTQATNRNTDGSTDYGILQINSRWWCND-
GRTPGSRNLCNIPCSALLSSDITASVNCAKKIVSDGNGMNAWVAWRNRCKGTDVQAWIRGCRL

pdb2xbr      KVFGRCELAAAMKRHGLDNYRGYSLGNWVCAAKFESNFNTQATNRNTDGSTDYGILQINSRWWCND-
GRTPGSRNLCNIPCSALLSSDITASVNCAKKIVSDGNGMNAWVAWRNRCKGTDVQAWIRGCRL

pdb2xth      KVFGRCELAAAMKRHGLDNYRGYSLGNWVCAAKFESNFNTQATNRNTDGSTDYGILQINSRWWCND-
GRTPGSRNLCNIPCSALLSSDITASVNCAKKIVSDGNGMNAWVAWRNRCKGTDVQAWIRGCRL

pdb2xjw      KVFGRCELAAAMKRHGLDNYRGYSLGNWVCAAKFESNFNTQATNRNTDGSTDYGILQINSRWWCND-
GRTPGSRNLCNIPCSALLSSDITASVNCAKKIVSDGNGMNAWVAWRNRCKGTDVQAWIRGCRL
```

Table 3: The PDB structures are clustered according to their resolution and their RMSD values. The nanobiotechnologies-based crystals are the most similar in the structural alignment and resolution (namely, APA-obtained and gold nanoparticles ones).

RMSD to 3iju	CRYSTALIZZATION TECHNIQUE	PDB STRUCTURES
0.13	Evaporation via gold nanoparticles	3p66
0.14	Evaporation via gold nanoparticles	3p65
0.14	Classical	3a8z
0.15	Sitting drops	3exd
0.15	Evaporation via gold nanoparticles	3p68
0.15	Classical	2xbr
0.16	Classical	2c8o, 2g4p
0.17	Batch	3ajn
0.17	Evaporation via gold nanoparticles	3p64
0.17	Classical	1lz9, 2c8p, 2w1x, 2w1y, 3kam
0.18	Classical	2w1l, 2hu3, 2w1m
0.19	Batch	1lz8
0.19	Capillary	2epe
0.19	Classical	2q0m, 2yvb, 193l, 1gwd
0.20	Space	1vds, 194l
0.20	Liquid-liquid diffusion	1jis, 3n9a, 3n9c, 3n9e
0.20	Classical	2htx, 1yil, 2hu1
0.20	Evaporation via gold nanoparticles	3p4z
0.21	Gel	1bvx
0.21	Sitting drops	1vat, 1vau
0.21	Space	1bwj
0.21	Classical	2h9j, 2h9k, 2xjw, 6lyt
0.22	Dialysis	1bwh
0.22	Classical	1azf, 1h6m, 2xth
0.23	Batch	1bwi
0.23	Classical	1t3p
0.24	Cryo-temperatures	2ydg
0.24	Classical	1t3p, 1h87, 2blx, 2d6b
0.25	Classical	1dpx, 2bpu
0.26	Classical	2a7d, 3b6l
0.27	Space	1vdt, 1iee
0.27	Classical	1lpi, 2zyp
0.29	Classical	1hew, 1uc0
0.31	Liquid-liquid diffusion	3qy4
0.31	Classical	1b0d, 2d91
0.33	Cryo-temperatures	1bhz
0.33	Classical	1hc0
0.35	Classical	2lyz, 3lyz, 8lyz
0.36	Classical	1lyo, 6lyz, 9lyz
0.40	Classical	3e3d
0.41	Classical	5lyt
0.47	Classical	4lyz, 5lyz
0.48	Classical	3ijv
0.52	Classical	1lyz

MD simulations confirm that the conformational and fluctuation dynamics of the two proteins differ: APA-grown lysozyme appears to be more flexible than its comparison.

As far as the elongated form of the APA crystal is concerned, taking into consideration the mathematical and physical analysis of Kondrat and Kornyshev (2011) [39], we can speculate that the differential crystal growth (namely, the particular ratio a/c reported above) can be explained taking

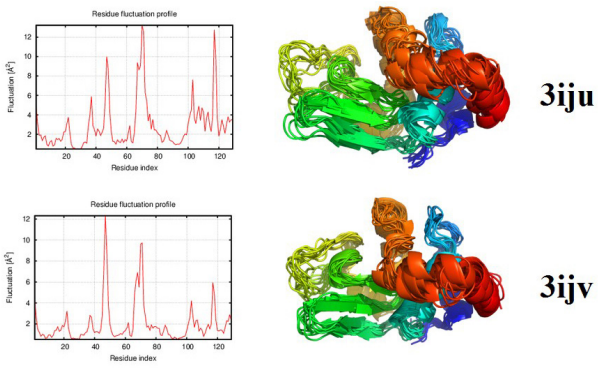

Figure 8: Molecular dynamics (MD) simulations of 3IJU and 3IJV carried out with CABS-flex server (as described in the text). APA-grown protein seems to be more flexible.

into account the electrostatic charge of the medium and its porous geometry. The kinetics is thus the resulting balance between two different contributing terms, namely the double-layer effect (positive term) and the pore shielded electrostatic attraction potential (negative term).

Conclusion

APA nanotemplate was prepared on the glass substrate for HEWL crystal growth by nanotemplate crystallization method. The changes in the lysozyme crystals morphology, namely the elongation as reflected in the *a/c* axis ratio, was observed in the crystal grown by APA nanotemplate, but not in the crystal grown by classical method, under the same experimental conditions. We compared the crystallographic and diffraction data, and we exploited bioinformatics approaches of data-mining and clustering as well as MD simulations in order to compare our crystals with all the other crystals deposited in PDB and made under the same experimental conditions.

Even though being structurally similar, as appeared from the data mining approach, the two proteins have different conformational and fluctuation dynamics, as shown by the MD analysis. Furthermore, from our bioinformatics analysis, we observed that APA-grown crystal does not cluster together with the classical one of comparison, but clusters instead with those structures obtained via nanobiotechnologies (specifically, the gold nanoparticles assisted *in situ* growth), suggesting a common biophysical/biochemical mechanism. In addition, from optical measurements carried out on over 100 crystal trials, we believe that the epitaxial growth we experimentally observed is induced by the APA template and can be due to the porous structure of the nanotemplate. In conclusion, APA appears capable to consistently influence the growth and design of protein crystal as shown in this communication for the lysozyme. Further implementation of the APA technology on nanocrystallography is discussed in the recent review article with details in the area of Nucleic Acid Programmable Protein Array (NAPPA) [40]. Further research will be needed to shed light on this topic, confirming and replicating our results, using also other model proteins.

Acknowledgments

This work was supported by grants to Fondazione EL.B.A. Nicolini (FEN) by MIUR (Ministero dell'Istruzione, Università e Ricerca) for "Funzionamento" 2011-2013 and by a FIRB Grant ITALNANONET from MIUR to Professor Dr. Claudio Nicolini of the Department of Experimental Medicine (DIMES) at University of Genoa and also to ESRF (European Synchrotron Radiation Facility). We thank Dr. Julie Ivy Trundley for the English revision of the manuscript.

References

1. Swaminathan R, Ravi VK, Kumar S, Kumar MV, Chandra N. 2011. Lysozyme: a model protein for amyloid research. Adv Protein Chem Struct Biol 84: 63-111. doi: 10.1016/B978-0-12-386483-3.00003-3.
2. Rosenberger F. 1996. Protein crystallization. J Crystal Growth 166(1-4): 40-54. doi: 10.1016/0022-0248(95)00921-3
3. Judge RA, Jacobs RS, Frazier T, Snell EH, Pusey ML. 1999. The Effect of Temperature and Solution pH on the Nucleation of Tetragonal Lysozyme Crystals. Biophys J 77(3): 1585–1593. doi: 10.1016/S0006-3495(99)77006-2
4. Schmit JD, Dill K. 2012. Growth rates of protein crystals. J Am Chem Soc 134(9): 3934-3937. doi: 10.1021/ja207336r
5. Tsekova J. 2009. Formation and Growth of Tetragonal Lysozyme Crystals at Some Boundary Conditions. Cryst Growth Des 9(3): 1312-1317. doi: 10.1021/cg800361v
6. Hirschler J, Fontecilla-Camps JC. 1996. Contaminant Effects on Protein Crystal Morphology in Different Growth Environments. Acta Crystallogr D Biol Crystallogr 52(4): 806-812. doi: 10.1107/S0907444996001813
7. McPherson A, Schlichta P. 1988. Heterogeneous and epitaxial nucleation of protein crystals on mineral surfaces. Science 239(4838): 385-387.
8. Georgieva DG, Kuil ME, Oosterkamp TH, Zandbergen HW, Abrahams JP. 2007. Heterogeneous nucleation of three-dimensional protein nanocrystals. Acta Crystallogr D Biol Crystallogr 63(5): 564-570. doi: 10.1107/S0907444907007810
9. Rong L, Komatsu H, Yoda S. 2002. Control of heterogeneous nucleation of lysozyme crystals by using Poly-L-Lysine modified substrate. J Crystal Growth 235(1-4): 489-493. doi: 10.1016/S0022-0248(01)01792-4
10. Falini G, Fermani S, Conforti G, Ripamonti A. 2002. Protein crystallisation on chemically modified mica surfaces. Acta Crystallogr D BiolCrystallogr 58(Pt 10 Pt 1):1649-1652. doi: 10.1107/S0907444902012763
11. Liu YX, Wang XJ, Lu J, Ching CB. 2007. Influence of the roughness, topography, and physicochemical properties of chemically modified surfaces on the heterogeneous nucleation of protein crystals. J Phys Chem B 111(50): 13971-13978. doi: 10.1021/jp0741612
12. Cvetkovic A, Straathof AJ, Krishna R, van der Wielen LA. 2005. Adsorption of xanthene dyes by lysozyme crystals. Langmuir 21(4):1475-1480. doi: 10.1021/la0478090
13. Kallio JM, Hakulinen N, Kallio JP, Niemi MH, Kärkkäinen S, et al. 2009. The contribution of polystyrene nanospheres towards the crystallization of proteins. PLoS One 4(1): e4198. doi: 10.1371/journal.pone.0004198
14. Rong L, Komatsu H, Yoshizaki I, Kadowakic A, Yoda S. 2004. Protein crystallization by using porous glass substrate. J Synchrotron Rad 11(1): 27-29. doi: 10.1107/S0909049503023525
15. Chayen NE, Saridakis E, EI-Bahar R, Nemirovsky Y. 2001. Porous Silicon: an Effective Nucleation-inducing Material for Protein Crystallization J Mol Bio. 312(4): 591-595. doi: 10.1006/jmbi.2001.4995
16. Ino K, Udagawa I, Iwabata K, Takakusagi Y, Kubota M, et al. 2011. Heterogeneous nucleation of protein crystals on fluorinated layered silicate. PLoS One 6(7):e22582. doi: 10.1371/journal.pone.0022582

17. Khurshid S, Saridakis E, Govada L, Chayen NE. 2014. Porous nucleating agents for protein crystallization. Nat Protoc 9(7): 1621-1633. doi: 10.1038/nprot.2014.109.
18. Chayen NE, Saridakis E, Sear RP. 2006. Experiment and theory for heterogeneous nucleation of protein crystals in a porous medium. PNAS 103(3): 597–601. doi: 10.1073/pnas.0504860102
19. Stolyarova S, Saridakis E, Chayen NE, Nemirovsky Y. 2006. A model for enhanced nucleation of protein crystals on a fractal porous substrate. Biophys J 91(10): 3857-3863. doi: 10.1529/biophysj.106.082545
20. Curcio E, Curcio V, Profio GD, Fontananova E, Drioli E. 2010. Energetics of protein nucleation on rough polymeric surfaces. J Phys Chem B 114(43): 13650-13655. doi: 10.1021/jp106349d
21. Pechkova E, Bragazzi NL, Nicolini C. 2014. Advances in nanocrystallography as a proteomic tool. Adv Protein Chem Struct Biol 95: 163-191. doi: 10.1016/B978-0-12-800453-1.00005-1.
22. Pechkova E, Nicolini C. 2001. Accelerated protein crystal growth onto the protein thin film. J Crystal Growth 231(4): 599-602. doi: 10.1016/S0022-0248(01)01450-6
23. Belmonte L, Pechkova E, Tripathi S, Scudieri D, Nicolini C. 2012. Langmuir-Blodgett nanotemplate and radiation resistance in protein crystals: state of the art. Crit Rev Eukaryot Gene Expr 22(3): 219-232. doi: 10.1615/CritRevEukarGeneExpr.v22.i3.50
24. Pechkova E, Vasile F, Spera R, Nicolini C. 2005. Protein nanocrystallography: growth mechanism and atomic structure of crystal induced by nanotemplates. J Synchrotron Rad 12(6): 772-778. doi:10.1107/S0909049505011647
25. Pechkova E, Sivozhelezov V, Tropiano G, Fiordoro S, Nicolini C. 2005. Comparison of lysozyme structures derived from thin film-based and classical crystals. Acta Crystallogr D Biol Crystallogr 61(6): 803-808. doi:10.1107/S0907444905006578
26. Pechkova E, Nicolini C. 2004. Protein nanocrystallography: a new approach to structural proteomics. Trends Biotechnol 22(3): 117-122. doi: 10.1016/j.tibtech.2004.01.011
27. Grasso V, Lambertini V, Ghisellini P, Valerio F, Stura E, et al. 2006. Nanostructuring of a porous alumina matrix for a biomolecular microarray. Nanotechnology 17(3): 795-798. doi: 10.1088/0957-4484/17/3/030
28. Stura E, Bruzzese D, Valerio F, Grasso V, Perlo P. 2007. Anodic porous alumina as mechanical stability enhancer for LDL-cholesterol sensitive electrodes. Biosens Bioelectron 23(5): 655-660. doi: 10.1016/j.bios.2007.07.011
29. Masuda H, Fukuda K. 1995. Ordered metal nanohole arrays made by a two-step replication of honeycomb structures of anodic alumina. Science 268(5216): 1466–1468. doi: 1t0.1126/science.268.5216.1466
30. Berman H, Westbrook J, Feng Z, Gilliland G, Bhat T, et al. 2000. The Protein Data Bank. Nucleic Acids Res 28: 235–242. doi: 10.1093/nar/28.1.235
31. Pechkova E, Bragazzi NL, Bozdaganyan M, Belmonte L, Nicolini C. 2014. A review of the strategies for obtaining high quality crystals utilizing nanotechnologies and space. Crit Rev Eukaryot Gene Expr 24(4): 325-339. doi: 10.1615/CritRevEukaryotGeneExpr.2014008275
32. Barthel D, Hirst JD, Blazewicz J, Burke EK, Krasnogor N. 2007. ProCKSI: a decision support system for Protein (Structure) Comparison, Knowledge, Similarity and Information BMC Bioinformatics 8: 416. doi: 10.1186/1471-2105-8-416
33. Zhang Y, Skolnick J. 2005. TM-align: a protein structure alignment algorithm based on the TM-score. Nucleic Acids Res 33(7): 2302-2309. doi: 10.1093/nar/gki524
34. Jamroz M, Kolinski A, Kmiecik S. 2013. CABS-flex: Server for fast simulation of protein structure fluctuations. Nucleic Acids Res 41(W1): W427-W431. doi: 10.1093/nar/gkt332
35. Durbin SD, Feher G. 1986. Crystal growth studies of lysozyme as a model for protein crystallization. J Crystal Growth 76(3): 583–592. doi: 10.1016/0022-0248(86)90175-2
36. Kim DT, Blanch HW, Radke CJ. 2002. Direct imaging of lysozyme adsorption onto mica by atomic force microscopy. Langmuir 18: 5841-5850. doi: 10.1021/la0256331
37. Mulheran P, Kubiak K. 2009. Protein adsorption mechanisms on solid surfaces: lysozyme-on-mica. Molecular Simulation 35(7): 561-566. doi: 10.1080/08927020802610288
38. Pechkova E, Tropiano G, Riekel C, Nicolini C. 2004. Radiation stability of protein crystals grown by nanostructured templates: synchrotron microfocus analysis. Spectrochim Acta Part B At Spectrosc 59(10-11): 1687-1693. doi: 10.1016/j.sab.2004.07.020
39. Kondrat S, Kornyshev A. 2011. Superionic state in double-layer capacitors with nanoporous electrodes. J Phys Condens Matter 23(2): 022201. doi: 10.1088/0953-8984/23/2/022201
40. Pechkova E, Chong S, Tripathi S, Nicolini C. 2009. Cell free expression and apa for NAPPA and protein nanocrystallography. Series on Nanobiotechnology (Series Editor C. Nicolini), Pan Stanford publishing, Vol 2.